Journal of ELECTRONIC MATERIALS, Vol. 39, No. 9, 2010
DOI: 10.1007/s11664-010-1190-8

Solar Thermoelectric Generator for Micropower Applications

R. AMATYA[1,2] and R.J. RAM[1]

1.—Research Laboratory of Electronics, Massachusetts Institute of Technology, 77 Massachusetts Avenue, Cambridge, MA 02139, USA. 2.—e-mail: ramatya@mit.edu

Solar thermoelectric generators (STG) using cheap parabolic concentrators with high-ZT modules can be a cost-effective alternative to solar photovoltaics for micropower generation. A thermodynamic analysis is presented for predicting the thermal-to-electrical conversion efficiency for the generator. With solar concentration of 66× suns, a system efficiency of 3% was measured for a commercial Bi_2Te_3 module with output power of 1.8 W. Using novel thermoelectric materials such as n-type ErAs:$(InGaAs)_{1-x}(InAlAs)_x$ and p-type $(AgSbTe)_x(PbSnTe)_{1-x}$, a conversion efficiency of 5.6% can be achieved for a STG at 120× suns.

Key words: Thermoelectric, solar, power generation

INTRODUCTION

Historically, thermoelectrics have been used primarily for deep-space exploration and waste heat recovery. We explore the potential of thermoelectrics with solar energy for electricity generation using a solar thermoelectric generator (STG) (Fig. 1a). A solar collector (parabolic reflector) directs the sunlight onto a fixed focal spot. The hot side of a thermoelectric generator placed at this spot heats up as it absorbs the concentrated sunlight. A "selective surface" on the hot side of the module has high (>90%) absorbance from 300 nm to 1000 nm.[1] This allows the hot side to absorb most of the incident solar energy. With appropriate selective surfaces most of the solar energy [ultraviolet (UV), visible, and infrared (IR)] incident on the generator contributes towards raising the hot-side temperature. A fraction of this thermal energy is converted to electrical energy by the thermoelectric module via the Seebeck effect. This paper provides a brief overview of the previous work in this field, followed by a presentation of new thermodynamic and cost models for STGs. Finally, experiments are used to validate the thermodynamic model; these experiments also realize record performance for STG modules.

(Received July 10, 2009; accepted March 8, 2010; published online April 3, 2010)

The first concept for a STG was tested in 1922 by Coblentz for measuring infrared radiation from stars.[2] Early work[2–5] showed low system efficiency (<1%), primarily due to low module ZT (<0.4), low solar concentration, and low hot-side temperature. To date, the highest measured efficiency for solar thermoelectrics is 3.35%, using a unicouple with ZT = 0.4 and solar concentration of 48× suns (1 sun = 1000 W/m^2).[2] The measured output power was 0.156 W. Figure 2 summarizes the previously published experimental results for different solar thermoelectrics, along with the experimental results presented at the end of this paper.

Complementing this experimental effort has been a history of STG modeling. A recently published model estimates a maximum system efficiency of 35% for a flat-plate (1× solar concentration) solar thermoelectric system.[6] Herein we show that the recently reported models are unphysical—specifically they treat the hot-side heat transfer inconsistently, resulting in hot-side temperatures of 900 K without solar concentration.[6] In fact, for a Bi_2Te_3 module with natural air convection, the heat flux at low solar concentration using flat-plate or box-type concentrators results in a relatively low hot-side temperature (<320 K).

THERMODYNAMIC MODEL

We present a thermodynamic analysis based on energy balance and heat transfer that allows us to

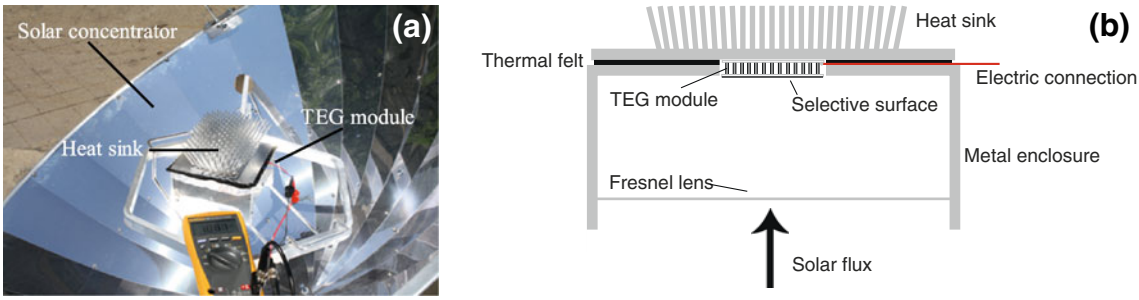

Fig. 1. (a) A solar thermoelectric generator, showing the concentrator and the heat sink. (b) Schematic of the enclosure holding the thermoelectric generator. A Fresnel lens is used to increase the flux concentration.

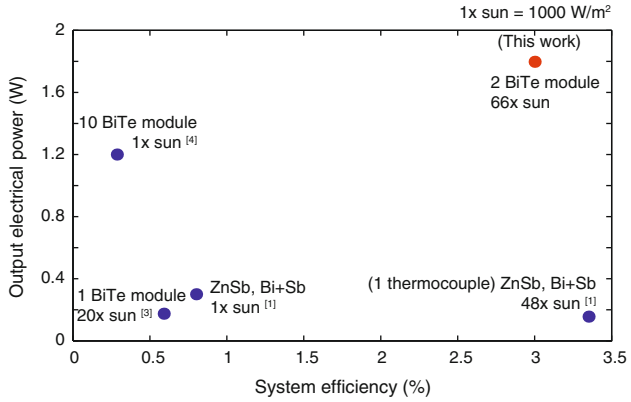

Fig. 2. Previous experiments for STG, shown with system efficiency and output electrical power.

predict system efficiency (η_{sys}) for the STG. The loss mechanism in the system can be categorized into two parts: loss in the concentrator and loss in the thermoelectric module. The concentrator efficiency (η_Q) is defined by how well the solar flux can be guided into the thermoelectric module. The efficiency is given by $\eta_Q = \frac{Q_h}{\phi_i A}$, where Q_h is the total thermal power into the thermoelectric generator (TEG), ϕ_i is the solar flux hitting the focal spot of the concentrator, and A is the area of the generator. The main losses degrading the concentrator efficiency are convective and radiative losses. The optical absorbance of the generator's hot side is also included in this efficiency. The module efficiency (η_{TEG}) depends on the thermoelectric material and the module design. It is given by $\eta_{TEG} = \frac{P}{Q_h}$, where P is the total electrical power generated, which depends on material properties such as the Seebeck coefficient, electrical conductivity, and thermal conductivity. For maximum power, the module efficiency can also be expressed by Eq. 1, where T_h is the hot-side temperature, T_c is the cold-side temperature, and ΔT is the temperature difference across the module. ZT_{module} is the figure of merit, which depends on the material parameters (Seebeck coefficient, thermal conductivity, and electrical conductivity) and module parasitics as described later in this paper.

$$\eta_{TEG} = \frac{\Delta T}{2T_h - \Delta T/2 + 2(T_h + T_c)/ZT_{module}}. \quad (1)$$

The total system efficiency is given by $\eta_{sys} = \eta_{TEG}\eta_Q$.

In general, convective loss can be reduced by introducing suppression mechanisms such as multiple glass panels and dead air between the glass and the hot side. In our experiment (Fig. 1b), the light hits the generator from below. An enclosure traps the warm air near the hot surface. This trapped air suppresses convective loss at the hot side. For radiative loss suppression, the hot side is coated with a selective surface consisting of silicon polymer as a binder with an oxide pigment.[1] The selective surface has a large absorbance (0.88 to 0.95) for visible wavelengths (300 nm to 1200 nm) and low emissivity (0.2 to 0.4) at wavelengths above 2.2 μm.[1] The selective surface allows for near-optimal absorption of incident solar radiation while minimizing radiative heat loss. Even at a relatively low hot-side temperature (<500 K), the selective surface performs better than ordinary black paint by increasing the overall temperature drop across the TEG by 10%.

STG performance was modeled using mature thermoelectric materials such as micro-alloy Bi_2Te_3 and SiGe, as well as novel materials with high material ZT (>1.2) such as ErAs:$(InGaAs)_{1-x}$-$(InAlAs)_x$[7] and $(AgSbTe)_x(PbSnTe)_{1-x}$.[8] Thermoelectric modules have relatively low effective ZT (0.25 to 0.4) compared with material ZT (Bi_2Te_3: $ZT \approx 1$), mostly due to thermal and electrical parasitics. Material ZT is given by $ZT_{material} = \left(\frac{\alpha^2}{R_{TE}K_{TE}}\right)T$, where α is the Seebeck coefficient, R_{TE} is the electrical resistance, and K_{TE} is the thermal conductance for a thermoelectric material. Module ZT can be formulated as $ZT_{module} = \left(\frac{\alpha^2}{(R_{TE}+R_{parasitic})(K_{TE}+K_{parasitic})}\right)T$, where $R_{parasitic}$ and $K_{parasitic}$ are the electrical parasitics (primarily metal interconnects between couples) and thermal parasitics (primarily ceramic plates for conventional designs). It can be seen from the above relationships that the module ZT is less than the material ZT due to parasitics. The module conversion efficiency is

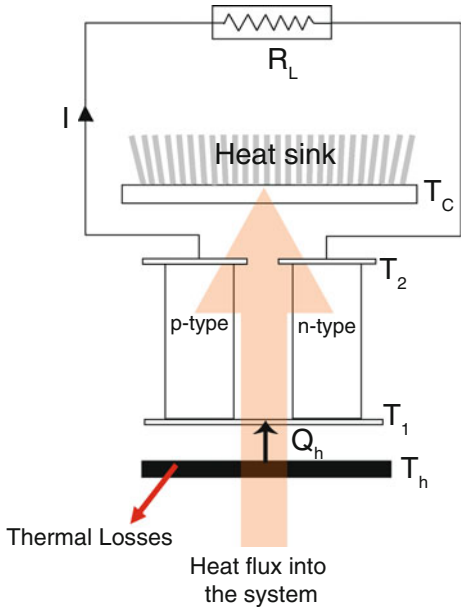

Fig. 3. Depiction of heat flux through the generator, showing various interfaces and temperatures.

determined by the module ZT rather than the material ZT.

For the simulation, the set of Eqs. 2–9 representing heat transfer and energy balance within the STG system (Fig. 3) is self-consistently solved for temperatures at various interfaces. The input solar flux (ϕ_i) is the only independent variable in the simulation. The cold-side heat transfer coefficient (h) is set by the natural air convection, which limits the cold-side temperature for the generator (T_c). The thermal impedance of the module sets the hot-side temperature for different heat flux. Depending on the temperature of the module (both hot and cold side), the generator efficiency is calculated. Both the convective and radiative losses at the hot side depend on the hot-side temperature.

$$Q_h = \eta_o \phi_i A - k_1(T_h - T_a)A - k_2 T_h^4 A, \quad (2)$$

where η_o is the optical absorbance for the hot-side absorber, k_1 is the convective heat transfer coefficient, k_2 is the radiative heat transfer coefficient, and T_a is the ambient temperature.

T_1 and T_2 are the temperatures across the material. Variations in these temperatures from T_h and T_c are due to the thermal parasitics, which are captured in the model as k_h and k_c—the hot-side and cold-side thermal conductance ($\sim$0.67 W/m^2 K).

$$Q_h = \frac{k_h(T_h - T_1)}{A}. \quad (3)$$

The total heat transported from the hot side can be separated into contributions from the Seebeck effect, thermal conductance, and Joule heating. α is the Seebeck coefficient of the TE material, which is temperature dependent. K is the thermal conductance, and R is the resistance of the module. I is the electrical current through the TEG.

$$Q_h = \alpha T_1 I + K(T_1 - T_2) - \frac{I^2 R}{2}. \quad (4)$$

Similarly, the total heat from the cold side is also due to the Seebeck effect, thermal conductance, and Joule heating:

$$Q_c = \alpha T_2 I + K(T_1 - T_2) + \frac{I^2 R}{2}. \quad (5)$$

The total electrical power generated by the TEG is then

$$P = Q_h - Q_c = \alpha(T_1 - T_2)I - I^2 R = I^2 R_L. \quad (6)$$

For maximum power, the condition of load matching is applied, according to which the load resistance (R_L) is equal to the resistance of the TEG (R), i.e.,

$$I = \frac{\alpha(T_1 - T_2)}{2R}. \quad (7)$$

The heat transfer at the cold side is given by Eqs. 8 and 9. A_{hs} is the area of the heat sink.

$$Q_C = \frac{k_C(T_2 - T_c)}{A}, \quad (8)$$

$$Q_c = hA_{hs}(T_c - T_a). \quad (9)$$

Using this analysis, Bi_2Te_3 with module ZT of 0.64 gives a system efficiency of 4% using natural air convection at the cold side with solar flux of 70$\times$ suns. In the thermodynamic analysis, the material properties (thermal conductivity, electrical resistivity, and Seebeck coefficient) are taken as temperature-dependent parameters. Figure 4 shows simulations of module ZT and system efficiency at various input solar fluxes. In this result, the existence of peak efficiency is due to the trade-off between the hot-side temperature and the material performance at high temperature: from Eq. 1, the module efficiency increases as the hot-side temperature rises. However, as the temperature increases, Bi_2Te_3's ZT degrades. The temperature of 900 K in Ref. 6 is not achievable primarily because the radiative loss (for $\varepsilon = 1$) exceeds the incident solar flux and because the material ZT for Bi_2Te_3 degrades at such high temperature.

EXPERIMENTAL PROCEDURES

Experiments were conducted using a Newport solar simulator (2 inch $\times$ 2 inch beam size) with commercial TEG modules. The average input thermal flux into the module was 66$\times$ suns, which was measured by using a thermopile sensor. This is

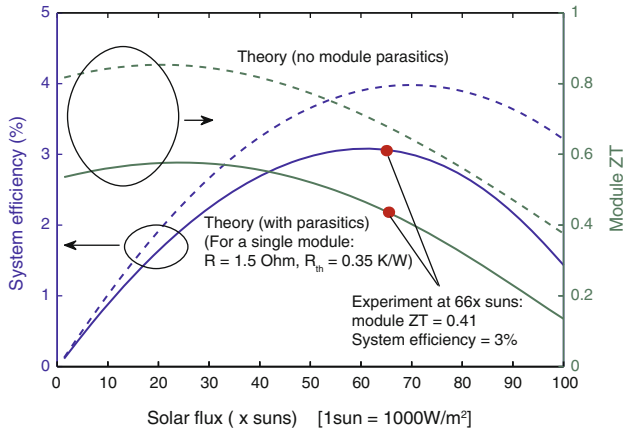

Fig. 4. Theoretical simulation for Bi_2Te_3, showing module *ZT* and system efficiency; without any parasitics, a maximum system efficiency of 4% is achieved at 70× suns. The model is verified with an experiment at 66× suns. Parasitics are included in the theory to represent the commercial module.

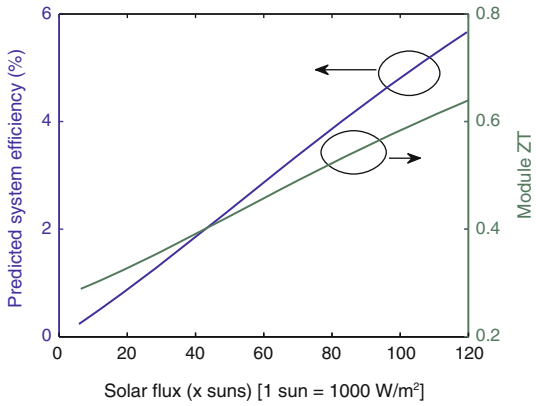

Fig. 5. Theoretical simulation for ErAs/LAST, showing system efficiency of 5.64% with module *ZT* of 0.64. The hot-side temperature is 700 K. Simulation was not done beyond this temperature, as the materials have not been tested at higher temperatures.

the input flux on the secondary concentrator, i.e., the Fresnel lens. The generator (TG12-4) from Marlow Inc., with a module $ZT \approx 0.41$[9] and material $ZT \approx 0.9$,[9] gave a system efficiency of 3% with output electrical power of 1.8 W. The generator was connected to a power metal–oxide–semiconductor field-effect transistor (MOSFET)-based variable resistance for load matching and maximum power measurement. An electrical parasitic of 1.5 Ω and thermal resistance of 0.35 K/W for the ceramic plates along with Bi_2Te_3 material parameters were used to model the commercial module. The experimentally measured system efficiency for the STG agrees with the thermodynamic model presented above. However, we can see that, even with greater solar concentration and with no module parasitics, the system efficiency with Bi_2Te_3 is limited to 4%. In order to realize higher efficiencies we must consider materials with high *ZT* at higher temperatures.

Novel thermoelectric materials such as *n*-type ErAs:$(InGaAs)_{1-x}(InAlAs)_x$[7] and *p*-type $(AgSbTe)_x$-$(PbSnTe)_{1-x}$,[8] have shown promising high material *ZT* (>1.2) for average temperatures in the range from 700 K to 750 K. Using this novel material combination, a system efficiency of 5.64% can be achieved with *ZT* of 0.64 (Fig. 4) at an average temperature of 546 K (Fig. 5). The solar concentration needed to reach an average temperature of 546 K is 120× suns. Simulations were not performed beyond a hot-side temperature of 700 K, as the materials have not been tested at these higher temperatures. Thus, for the simulation, *ZT* never reaches the highest value of 1.2. The thermodynamic model, even with novel materials, suggests that system efficiencies of 6% are beyond the reach of STGs. However, even with these modest efficiencies, STGs may be of commercial interest if the overall system cost can be kept sufficiently low.

COST MODEL

In this final section, we present a cost model for the STG, comparing it with photovoltaics (PV). The bulk retail price for a 15-W thermoelectric generator is US $25,[10] giving a peak power price of US $1.67/$W_p$, whereas the retail peak power price for a PV module is US $4/$W_p$ at the time of publication.[11] This PV price includes installation cost. Both TEG and PV have similar lifetime (15 years to 20 years) and low maintenance cost. The electronic circuit requirements are also similar for PV and TEG, as both require batteries, charge controllers, inverters, etc. The critical difference is the conversion efficiency, which is between 7% and 12% for a low-cost PV module. Commercial TEG modules are rated for 4% optimum conversion efficiency for a large temperature difference (T_H = 230°C, T_C = 50°C).[9] A low-cost parabolic concentrator can focus a solar flux of ~10× suns on a spot size of 28 cm diameter. Using inexpensive Fresnel lenses as secondary concentrators, the flux can be easily increased to 50× to 150× suns. The electricity price (US ¢/kW h) for the STG was calculated using the total amount of electrical power generated within the lifetime of a generator (20 years). The generator efficiency, $\eta(\phi_i)$, depends on the incident solar flux (ϕ_i) as shown in Fig. 6.

The output power at any given instant is equal to the system efficiency multiplied by the total thermal power incident on the generator. The thermal power into the generator depends on the incident solar flux and the generator area (*A*), as well as on radiative and convective losses from the absorber surface. Figure 6 also shows the total number of hours in a year (P_{ϕ_i}) that solar radiation of a certain intensity hits the Earth's surface. The yearly average for this particular location (Kathmandu, Nepal) is 210 W/m^2. The total output power within the lifetime of a generator is given by the sum of output power for each hour of the day as shown in Eq. 10.

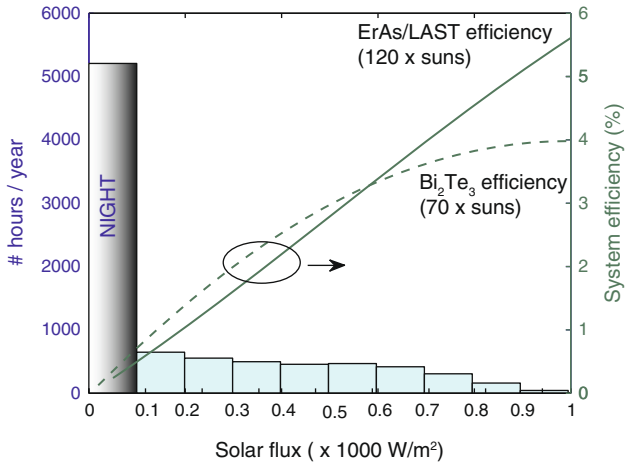

Fig. 6. Dependence of system efficiency on solar flux for Bi_2Te_3 and ErAs/LAST material. The total number of hours within a year for certain flux radiation is also shown as a histogram.

$$\langle P_{\text{electrical}} \rangle = \left(\sum_{\text{i}} \eta(\phi_{\text{i}}) \times \phi_{\text{i}} \times A \times P_{\phi_{\text{i}}} \right) \times 20. \quad (10)$$

Table I shows the electricity price with the STG using various thermoelectric materials.

We explore the effect of parasitics on the electricity pricing. At fixed solar concentration, the module ZT is varied by introducing electrical parasitic resistance (0 Ω to 5 Ω). As the parasitic increases, the module ZT and the system efficiency decrease. When the system efficiency decreases, the electricity price rises. Figure 7a shows the price dependence for Bi_2Te_3. Simulations with two different geometrical aspect ratios, i.e., cross-section/length, of 0.56 cm and 0.2 cm for the TE leg show that the modified Bi_2Te_3 module with low parasitics and longer TE legs can have electricity price comparable to the PV price. For higher solar concentration and the ErAs/lead-antimony-silver-tellurium (LAST) combination, even with the aspect ratio of 0.56 cm, which is the aspect ratio for a commercial module, the system efficiency is high enough for the electricity cost to be within the PV price range (Fig. 7b).

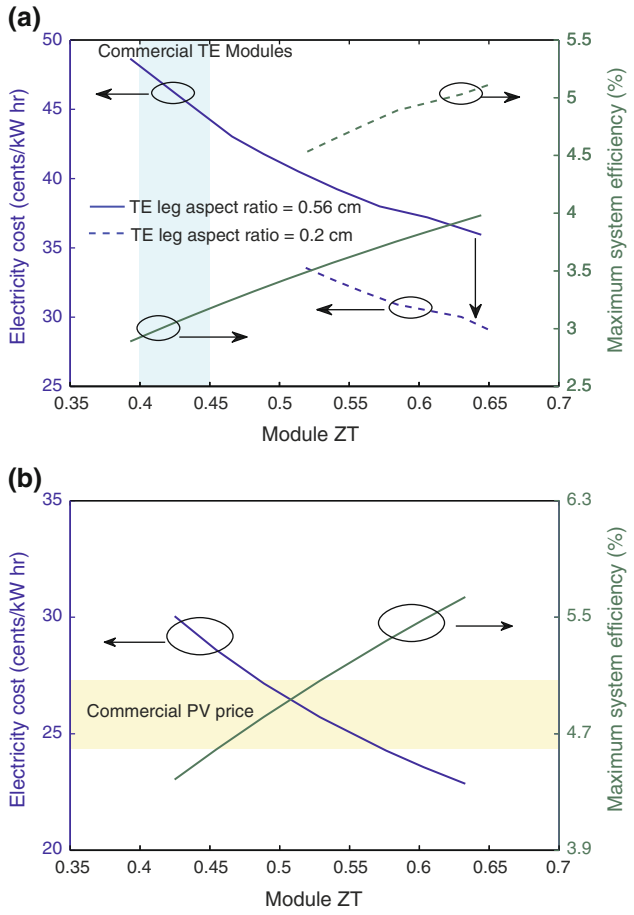

Fig. 7. (a) Electricity cost variation in Bi_2Te_3 by changing module parasitic resistance at 70× suns. As the resistance increases, the module ZT decreases. With a modified module design (longer TE legs), the system efficiency can be increased to decrease the electricity cost. (b) By choosing higher solar concentration (120× suns) and materials such as ErAs/LAST, the electricity cost is within 22 US ¢/kW h to 30 US ¢/kW h.

CONCLUSIONS

In this work, we have presented experimental and theoretical results relating to solar-to-electrical conversion using thermoelectrics. Generators employing light concentrators and modules with high-ZT thermoelectric materials are an attractive alternative to solar photovoltaics for micropower applications. We can predict conversion efficiency for a STG using various materials at different temperature ranges using a thermodynamic analysis based on energy balance and heat transfer. With novel thermoelectric materials which have high material ZT, a system efficiency of 5.6% can be achieved. Experimentally we show a system efficiency of 3% with a commercial Bi_2Te_3 module, which is (to the best of our knowledge) the highest

Table I. Price of electricity for a STG using various thermoelectric materials compared with PV

Material	ZT (module)	Max. System Efficiency (%)	Solar Concentration	Average Temperature (K)	Electricity Price (US ¢/kW h)
Bi_2Te_3	0.64	4	70× suns	446	35
ErAs/AgSbTe	0.64	5.64	120× suns	546	22
Si (PV)	–	11	–	–	20–26[11]

efficiency for solar thermoelectrics using a module. From the cost analysis perspective, even though present-day commercial modules have low module ZT ($\sim$0.4) and low system efficiency, the thermoelectric element geometry can be optimized for performance in the STG application. With better module design (longer TE legs and low parasitics), and by using materials with improved thermoelectric properties at higher temperature, solar thermoelectrics can be economically competitive with small-scale PV power generation for many applications such as rural electrification in developing countries and power supply for remote sensors.

REFERENCES

1. SOLKOTE: HI/SORB-II Selective Solar Coating (NJ, USA: Solec Inc.). http://www.solec.org.
2. M. Telkes, *J. Appl. Phys.* 25, 765 (1954).
3. N. Vatcharasanthien, J. Hirunlabh, J. Khedari, and M. Daguenet, *Int. J. Sustain. Energy* 24, 115 (2005).
4. S.A. Omer and D.G. Infield, *Sol. Energy Mater. Sol. C* 53, 67 (1998).
5. H. Xi, L. Luo, and G. Fraisse, *Renew. Sustain. Energy Rev.* 11, 923 (2005).
6. J. Chen, *J. Appl. Phys.* 79, 5 (1996).
7. G. Zeng, J. Bahk, J.E. Bowers, J.M.O. Zide, A.C. Gossard, Z. Bian, R. Singh, A. Shakouri, W. Kim, S.L. Singer, and A. Majumdar, *Appl. Phys. Lett.* 91, 263510 (2007).
8. A. Kosuga, K. Kurosaki, H. Muta, and S. Yamanaka, *J. Alloys Compd.* 416, 218 (2006).
9. TG 12-4 (TX, USA: Marlow Inc.). http://www.marlow.com.
10. Thermonamic Electronics (Xiamen) Co. Ltd., Xiamen Taihuaxing Trading Co., Ltd (Marketing Office), West Unit 309, Guang Ye Building, Torch Hi-Tech Industrial Development Zone, Xiamen, China 361006.
11. Solarbuzz LLC, USA. http://www.solarbuzz.com.